Colloid Polym Sci (2011) 289:1769–1776
DOI 10.1007/s00396-011-2493-x

SHORT COMMUNICATION

Co-effect of soft template and microwave irradiation on morphological control of gold nanobranches

Yun Fang · Yueping Ren · Ming Jiang

Received: 19 May 2011 / Revised: 5 July 2011 / Accepted: 2 August 2011 / Published online: 6 September 2011

Abstract Short-range order sodium dodecyl sulfate (SDS)-bound micelles and long-range order poly(vinylpyrrolidone) (PVP)–SDS supramolecular assemblies in PVP–SDS aqueous solution illustrate the potential template application in directing hierarchical assembly of inorganic nanostructure. In this paper, ginger-like Au nanobranches with equivalent circle diameter around 50 nm were prepared in PVP–SDS aqueous solution under microwave irradiation through a one-pot, facile, rapid, and morphology-controlled synthesis route. Based on the experimental results, the possible growth mechanism of the ginger-like gold nanobranches is inferred to be a template-mediated and microwave-assisted hierarchical assembly via the unique co-effect of PVP–SDS soft template and microwave irradiation. At first, the precursors $AuCl_4^-$ surrounding the SDS-bound micelles were rapidly reduced to Au^0 by sodium citrate assisted by microwave irradiation and simultaneously assembled into abundant Au nanocrystals with diameters around 10 nm according to the bound micelle templates. And then several tiny Au nanocrystals linked by PVP chains within a limited space were instantly mediated by the long-range order PVP–SDS supramolecular assemblies to fabricate into polycrystal ginger-like Au nanobranches. X-ray diffraction (XRD) pattern indicates that the Au nanobranches are face-centered cubic phase, which is verified by high-resolution transmission electron microscopy (HRTEM) images and selected area electron diffraction (SAED) pattern.

Keywords Gold · Nanobranches · Hierarchical assembly · Microwave irradiation · Soft template · Poly (vinylpyrrolidone)

Y. Fang (✉) · M. Jiang
Key Laboratory for Molecular Engineering of Polymers, Ministry of Education, Department of Macromolecular Science, Fudan University,
Shanghai 200433, People's Republic of China
e-mail: yunfang@126.com

Y. Fang · Y. Ren
School of Chemical and Material Engineering, Jiangnan University,
Wuxi, Jiangsu 214122, People's Republic of China

Introduction

The morphology-controlled synthesis of gold nanostructures has attracted extensive research interests because of their unique shape-dependent properties and widespread applications [1, 2]. In the past few years, gold nanospheres [3], nanorods [4], nanowires [5], nanoplates [6], and nanocubes [7] have been successfully synthesized. Recent studies have shown that the local electromagnetic field at the tips of branched gold nanoparticles was intensely enhanced which made them attractive for use as surface-enhanced Raman scattering (SERS) substrates [8]. Therefore, great interests have been focused on the preparation and application of branched gold nanoparticles. By far, the previous reports for the synthesis of branched nanoparticles were mainly based on a seed-mediated growth approach [9–11]. For example, Khoury et al. [12] reported the seed-mediated synthesis of gold nanostars in DMF medium by using poly(vinylpyrrolidone) (PVP) as capping agent. Kuo et al. [13] synthesized gold nanobranches through a stepwise procedure by using sodium dodecyl sulfate (SDS) as capping agent. Wu et al. [14] prepared elongated penta-branched gold nanocrystals with a shape resembling that of a star fruit but with sharp ends by a multistep seeding growth approach. Therefore, developing a facile, no seeding, and high-yield method that is using common

capping agents and operating in aqueous solutions for the synthesis of branched nanoparticles is highly desirable. PVP is widely used as capping agent *cum* reductant in the synthesis of two-dimensional noble metal nanostructures [15, 16]. Moreover, it is reported that PVP can interact with anionic surfactant SDS to form PVP–SDS supramolecular assemblies [17, 18]. These supramolecular assemblies are ideal templates for the synthesis of various nanostructures because their combinatorial structures are totally different from that of pure surfactants or pure water-soluble polymers [19, 20] which inspire us to explore the using of PVP–SDS aqueous solution for the synthesis of gold nanostructures. In this paper, ginger-like gold nanobranches with high yield and good size monodispersity were synthesized in PVP–SDS aqueous solution assisted by microwave irradiation. Comparing with ordinary heating, the microwave-assisted synthesis is faster, simpler, and more energy efficient [21, 22].

Experimental

Materials

$HAuCl_4$ and sodium citrate were purchased from Sinopharm Chemical Reagent Co. Ltd., China. SDS was purchased from Acros Organics Co., USA. PVP K30 was granted by International Specialty Products, Inc. All reagents were used as received without further purification, and ultra pure water was used throughout.

Surface tension measurements

The surface tension (γ) of the pure SDS, PVP–SDS, $HAuCl_4$–SDS, and $HAuCl_4$–PVP–SDS solutions was measured by Wilhelmy method at 25 °C using surface tension instrument DCA 315 (Thermo Cahn). The concentrations of PVP and $HAuCl_4$ were 1 $g \cdot L^{-1}$ and 0.3 mM, respectively, which were uniform in all the solutions.

Synthesis

In a typical experiment, 1.25 mL PVP (20 $g \cdot L^{-1}$), 5 mL SDS (50 mM), and 0.75 mL $HAuCl_4$ (10 mM) were added to a 25 mL volumetric flask, and the volume was then adjusted to 25 mL with water; the final concentrations of PVP, SDS, and $HAuCl_4$ were 1 $g \cdot L^{-1}$, 10 mM, and 0.3 mM, respectively. The mixed solution was transferred into a conical flask and to be heated in a domestic microwave oven (200 W) until boiling. And then, the solution continued boiling for 5 min after 1 mL aqueous solution of sodium citrate (85 mM) was added into it rapidly.

Characterization

Transmission electron microscopy (TEM) images were obtained on a Hitachi H-70000 transmission electron microscope. High-resolution transmission electron microscopy (HRTEM) image and the corresponding selected area electron diffraction (SAED) pattern were obtained with a JEOL 2010 high-resolution transmission electron microscope operated at an accelerating voltage of 200 kV. XRD was carried out with a D/Max 2500 X-ray diffractometer using Cu (40 kV, 200 mA) radiation. The surface plasma resonance (SPR) was recorded on PGENERAL TU-1901 spectrophotometers.

Results and discussion

Characterization of ginger-like gold nanobranches

XRD pattern (Fig. 1a) of the as-synthesized gold nanostructures shows that the sample is face-centered-cubic phase. Five peaks observed in the 2θ range of 30–85° can be indexed, respectively, to (111), (200), (220), (311), and (222) reflections of gold. It is worth noting that the ratio of the intensity between the (200) and the (111) diffraction peaks ($I_{(200)}/I_{(111)}$) is much lower than the standard file (0.28 versus 0.52). These observations confirm that the obtained gold nanostructures are primarily dominated by (111) facets [13, 23]. The TEM image shown in Fig. 1b indicates that the as-synthesized nanostructures are ginger-like gold nanobranches. These nanobranches are 50 nm in size, and each of them possesses several convex bumps. Four typical ginger-like gold nanobranches are shown in Fig. 1c which are similar to that reported by Kuo et al. [13]. In their route, SDS with an exorbitant concentration (50 mM) was used as capping agent, and the entire process prolonged for about 1 h. Figure 1d is the SPR characteristics of the obtained ginger-like gold nanobranches. Except the strong SPR peak around 533 nm, there is a protuberant absorption band in 600–700 nm. The appearance of this broad plasmon peak is mainly because their tip lengths vary widely within a single nanobranch and among different nanobranches [24].

The HRTEM image of a single ginger-like gold nanobranch shown in Fig. 2a reveals that the measured fringe spacings are all 0.235 nm which equates with the (111) lattices spacing of gold crystals, but the lattice orientation depends on the location on a gold nanobranch. Figure 2b, c shows the HRTEM images of the concave parts on the gold nanobranch marked with “A” and “B” in Fig. 2a. The lattice orientations between the adjacent parts are different, and the angles of them are 43° and 35°, respectively (Fig. 2b, c). The electron diffraction spots in the SAED

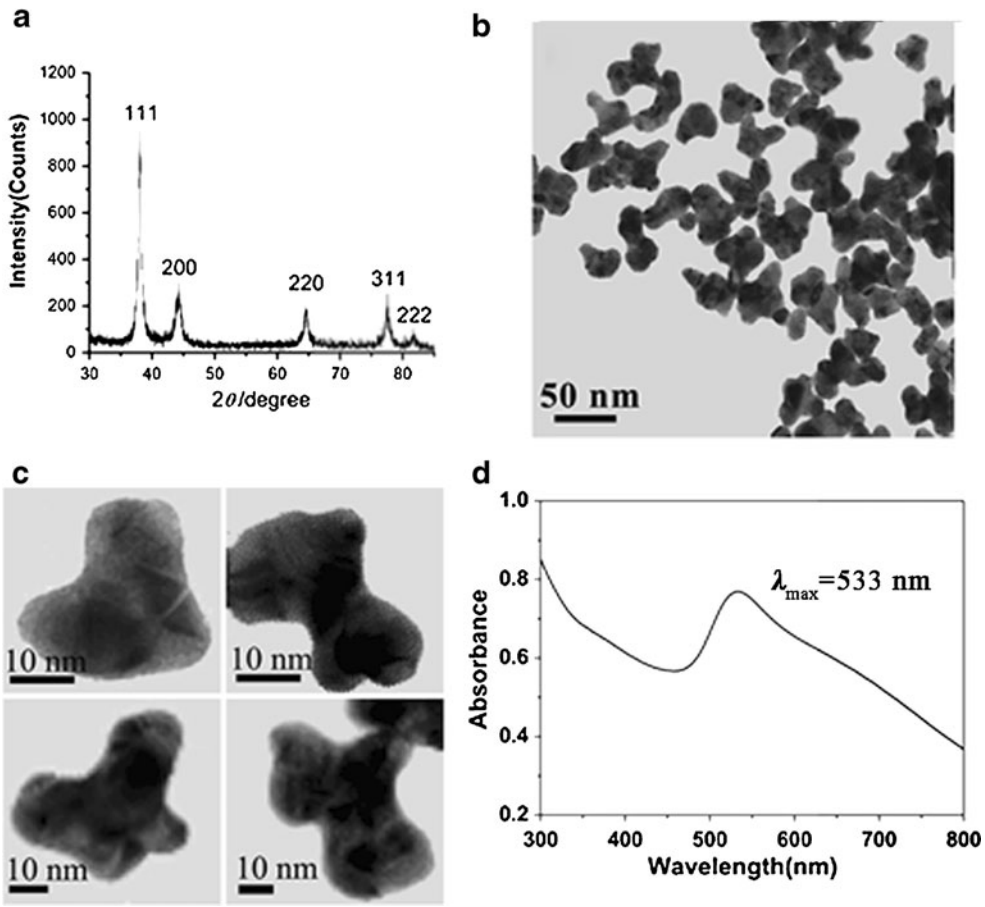

Fig. 1 Characterization of ginger-like gold nanobranches obtained under microwave irradiation in 10 mM of SDS, 1 $g \cdot L^{-1}$ of PVP, and 0.3 mM of $HAuCl_4$: **a** XRD pattern, **b** TEM image, **c** enlarged TEM images, and **d** SPR characteristics

pattern of a single gold nanobranch arrange as a circle which suggests that the gold nanobranches are not single crystals (Fig. 2d). It is reasonable to conclude that these ginger-like gold nanobranches are fabricated by a few tiny gold nanocrystals in random lattice orientation.

TEM images of gold nanoparticles synthesized in PVP–SDS aqueous solution at different SDS concentrations are shown in Fig. 3. Quasi-spheric gold nanoparticles, which are 10–20 nm in size as shown in Fig. 3a are synthesized in blank sample without SDS. When a little SDS was added (0.2 mM), the synthesized products in Fig. 3b were still quasi-spheres, and it is interesting that these quasi-spheres rounded in cycles with diameters of 200–300 nm to reduce their exorbitant surface energies [25]. The enlarged TEM image in the illustration of Fig. 3b shows the size monodispersity of gold nanoparticles is excellent. Increasing SDS concentration to 3 mM, lots of tri-branched gold nanoparticles appeared, and some elongate nanoparticles coexisted as byproducts as shown in Fig. 3c. As SDS concentration continued to increase to 8 mM, the synthesized nanoparticles in Fig. 3d were ginger-like gold nanobranches of 40–50 nm in size and tri-branched or tetra-branched in

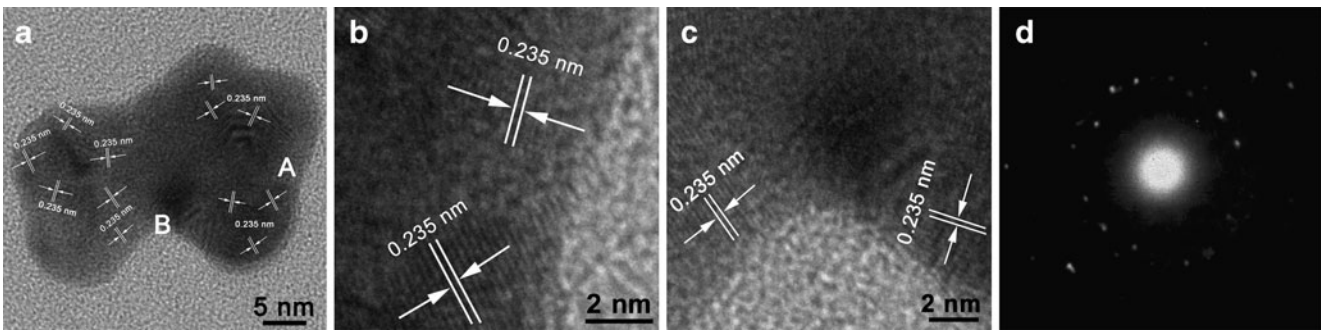

Fig. 2 Crystal structure characterization of ginger-like gold nanobranches obtained under microwave irradiation in 10 mM of SDS, 1 $g \cdot L^{-1}$ of PVP, and 0.3 mM of $HAuCl_4$: **a** HRTEM image of entire ginger-like gold nanobranches, **b** concave part A in (a), **c** concave part B in (a), and **d** SAED pattern of single ginger-like gold nanobranches

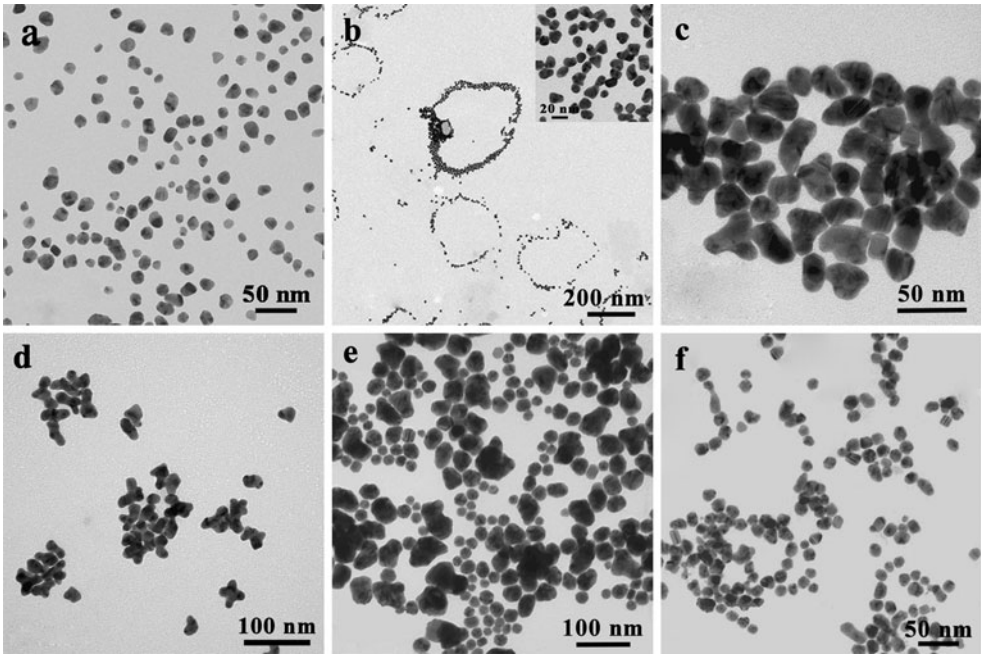

Fig. 3 TEM investigation of the template function for gold nanostructures obtained under microwave with 1 $g \cdot L^{-1}$ of PVP and 0.3 mM of $HAuCl_4$ and in different concentrations of SDS: **a** 0, **b** 0.2, **c** 3, **d** 8, **e** 15, and **f** 30 mM

shape, which much resembled those shown in Fig. 1b obtained at SDS concentration of 10 mM. However, at SDS concentration of 15 mM, the synthesized products shown in Fig. 3e were mixtures of large irregular nanoparticles of 60 nm in size and small quasi-spheres of 20 nm in size. At higher SDS concentration (30 mM), the synthesized products shown in Fig. 3f return to all quasi-spheres of 15–20 nm in size.

Because good shape stability is the precondition for the subsequent application of nanoparticles, the shape stability of quasi-spheres in Fig. 3b and typical ginger-like gold nanobranches in Fig. 3d were laid up 2 months at 30 °C, and the corresponding TEM images are shown in Fig. 4. Compared with the corresponding TEM images in Fig. 3b, the circles assembled by quasi-spheres disappeared, and the ring-like fabrications redistributed to single quasi-spheres as shown in Fig. 4a. Taking account of ginger-like gold nanobranches in Fig. 3d, there are no obvious morphology variations in Fig. 4b after standing 2 months, which suggests that the ginger-like gold nanobranches have enough stability for the subsequent application in case.

The influences of SDS concentration on the morphologies of the synthesized gold nanoparticles are attributed to the variations of the organized molecular assemblies in PVP–SDS aqueous solution at different SDS concentrations. According to previous reports, there is strong interaction between SDS and PVP in aqueous solution [26]. Figure 5a shows the γ-lg c_{SDS} curve of $HAuCl_4$–PVP–SDS aqueous solution versus logarithm of the concentration of SDS (c_{SDS}) which exhibits two turning points. The first one is related to the beginning binding of surfactant to polymer, defined as CAC or c_1. The second point is the outset forming of SDS free micelles which is called polymer saturation point or the second critical concentration (c_2) [27]. Between c_1 and c_2 in $HAuCl_4$–PVP–SDS aqueous solution, PVP and SDS self-assemble into supramolecular assemblies with three-dimensional pearl-necklace-like structure in which SDS-bound micelles serve as pearls and PVP chains as strands [17, 28]. Therefore, SDS concentration is a key influence factor dominating the variations of the organized molecular assemblies of PVP and SDS which would certainly exert further dramatic template influences on morphologies of gold nanoparticles.

It was reported that PVP, SDS monomers, SDS micelles, and PVP–SDS aggregates are all effective templates for synthesizing inorganic nanomaterials in liquid-phase method [29–31]. Free SDS micelles help to protect nascent nanocrystals growing into tiny nanoparticles [32]. And PVP chains could absorb onto gold facets with the oxygen atom in the pyrrole unit [33]; nascent gold nanocrystals, therefore,

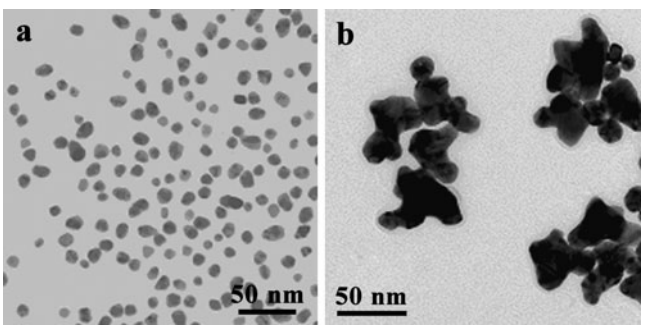

Fig. 4 TEM image of gold nanoparticles after standing at 30 °C for 2 months. **a** Quasi-spheres and **b** ginger-like gold nanobranches

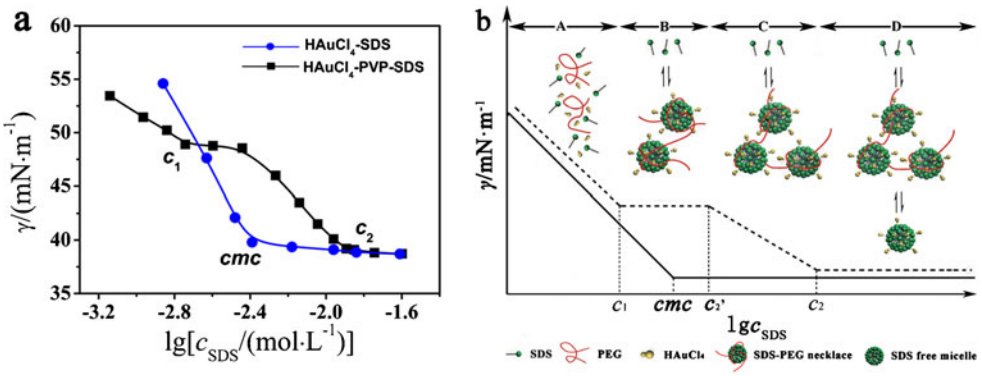

Fig. 5 **a** γ-lg c_{SDS} curves of $HAuCl_4$–SDS and $HAuCl_4$–PVP–SDS aqueous solutions with 1 $g \cdot L^{-1}$ of PVP and 0.3 mM of $HAuCl_4$ and **b** schematic presentation of the relationship between SDS concentration and equilibrium of template species

are stabilized by PVP in aqueous solution, and after Ostwald ripening, they are easy to grow into small quasi-spheres. However, in PVP–SDS supramolecular assemblies, PVP chains were occupied by SDS-bound micelles which weaken the protecting effect of PVP on nascent nanocrystals so that the nascent nanocrystals trend to somewhat aggregate to form larger fabricated nanostructures to lower their exorbitant surface energy [34]. Altering SDS concentration in $HAuCl_4$–PVP–SDS aqueous solution should be the most fruitful approach to provide different type of templates in a single system. In the experimental $HAuCl_4$–PVP–SDS aqueous solution in the presence of 1 $g \cdot L^{-1}$ of PVP and 0.3 mM of $HAuCl_4$, the c_1 and c_2 values are 1.8 and 12.8 mM, respectively. The equilibrium of template species in $HAuCl_4$–PVP–SDS aqueous solution is shown in Fig. 5b. PVP and SDS monomers are main template species when SDS concentration is lower than 1.8 mM that refers to the c_1 value, and free SDS micelles would become the main template species in turn when SDS concentration is beyond 12.8 mM that refers to the c_2 value. It is worth paying special attention to the fire-new template species appearing when SDS concentration is between 1.8 and 12.8 mM, the three-dimensional pearl-necklace-like aggregates composed of SDS molecules and PVP chains. The picture of short-range order SDS-bound micelles and long-range order PVP–SDS supramolecular assemblies illustrates the potential template application of PVP–SDS aqueous solution in directing hierarchical assembly of inorganic nanostructure. Therefore, the two critical concentrations of SDS in $HAuCl_4$–PVP–SDS aqueous solution, c_1 and c_2, are the threshold concentrations to control nanoparticle morphology, which is very helpful to explain why various nanoparticle morphologies appeared and depend on the SDS concentration variations.

Co-effect of soft template and microwave irradiation on morphology

To clearly illustrate the co-effect of soft template and microwave irradiation on morphological control of gold nanobranches, the function of the different templates of SDS, PVP, or PVP–SDS supramolecular assemblies under microwave irradiation was investigated, respectively; thus, the corresponding dominant synthesized products are both quasi-spheres in SDS or PVP aqueous solutions alone but typical ginger-like gold nanobranches in PVP–SDS supramolecular assemblies as shown in Fig. 6a–c. Figure 6d shows the corresponding XRD patterns of the ginger-like gold nanobranches synthesized in PVP–SDS supramolecular assemblies and the gold quasi-spheres synthesized in SDS or PVP solutions. The diffraction peak intensities of the gold quasi-spheres are remarkably lower than that of the gold nanobranches, especially the intensity of the (111) diffraction peaks, which revealed that the crystalline of the ginger-like gold nanobranches is superior to the gold quasi-spheres. Therefore, although the microwave irradiation accelerates and disturbs the synthesis process, PVP–SDS

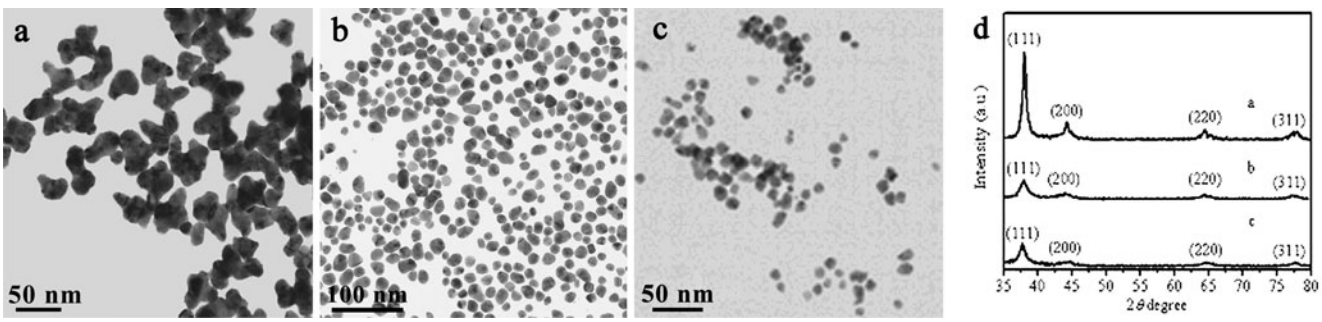

Fig. 6 TEM images of gold nanostructures (0.3 mM of $HAuCl_4$) obtained under microwave in **a** PVP (1 $g \cdot L^{-1}$)–SDS (10 mM), **b** SDS (10 mM), **c** PVP (1 $g \cdot L^{-1}$), and **d** their corresponding XRD patterns

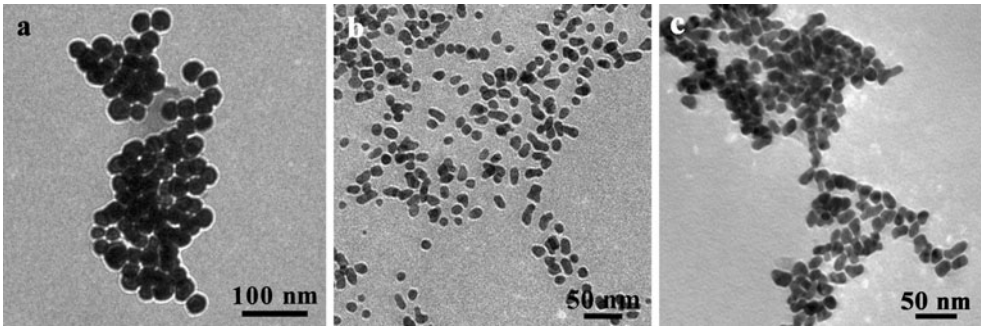

Fig. 7 TEM images of gold nanostructures (0.3 mM of $HAuCl_4$) obtained under ordinary heating in **a** SDS (10 mM), **b** PVP (1 $g \cdot L^{-1}$), and **c** PVP (1 $g \cdot L^{-1}$)–SDS (10 mM)

supramolecular assemblies still exert better template effect on orderly crystal growth of nanocrystals than SDS or PVP does.

The above soft templates were also examined under ordinary heating to eliminate the influence of microwave irradiation; thus, the corresponding dominant synthesized products are, respectively, nanospheres, elongate nanoparticles, or mixtures of elongate nanoparticles and little nanobranches as shown in Fig. 7. The experimental results show that the occurrence of PVP facilitated the directed aggregation of nanocrystals to enlarged or elongate nanoparticles due to its random coil structure in aqueous solution, while the PVP–SDS supramolecular assemblies have the function to direct nanocrystals further elongated and even branched to result in nanobranches due to its unique three-dimensional necklace-like structure. It is also easy to find by comparing Fig. 6 with Fig. 7 that microwave irradiation is in favor of promoting irregular morphology.

Based on these results, a tentative explanation on the coeffect of soft template and microwave irradiation on morphological control of gold nanobranches is proposed. Firstly, compared with PVP itself, the protecting effect of PVP–SDS supramolecular assemblies are weaker since PVP chains have been occupied by SDS-bound micelles, and in this case, the nascent gold nanocrystals as a whole trend to aggregate to lower their exorbitant surface energy. Secondly, PVP–SDS supramolecular assemblies have stronger potential to fabricate tiny gold nanocrystals into elaborate gold nanostructures than the single-component templates anyhow with or without microwave assistance that is because the PVP–SDS supramolecular assemblies themselves have the hierarchical structure in favor of direct hierarchical assembly of gold nanocrystals. In the process of hierarchical assembly of gold nanobranches, the short-range order SDS-bound micelles could act as the primary templates to mediate the tiny nanocrystals with diameters around 10 nm according to the micelle templates; one after the other, the long-range order PVP–SDS aggregates could act as the secondary templates to fabricate several above gold nanocrystals linked by PVP chains within a limited space into elaborate gold nanostructures. Thirdly, microwave irradiation could offer more rapid and uniform heating to all solvents, reagents, and intermediates than ordinary heating [35], so that abundant nascent gold nanocrystals occur in the initial stage of the reaction which is the precondition to fabricate gold nanobranches subsequently. Microwave irradiation should disturb and weaken the original template function of capping agents and result in an elevated disorder lever of the gold nanoparticles in some extent that is why, we think, microwave irradiation is in favor of promoting irregular morphology. The last but not the least, there is an interaction between somewhat disorderly accelerating effect resulting from microwave

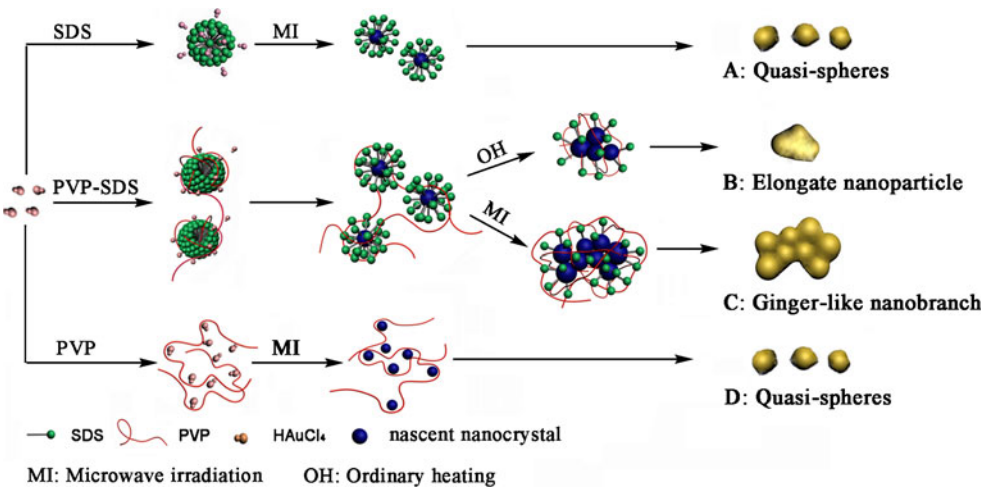

Fig. 8 Schematic mechanism of template-mediated and microwave-assisted hierarchical assembly of ginger-like gold nanobranches

irradiation and a hierarchically assembling template function provided by PVP–SDS supramolecular assemblies. It is the unique co-effect of soft template and microwave irradiation that promotes those gold nanocrystals occurred in the initial stage of the reaction in high concentration more apt to aggregate to fabricate ginger-like gold nanobranches. Moreover, since microwave irradiation has expressed the potential to promote zigzag, branched, corolliform, and rough morphological characteristics, it can yet be regarded as the assistance means to provide SERS "hot spot" in synthesizing other nanomaterials [36].

Proposed growth mechanism of gold nanostructures

The proposed growth mechanism of different nanostructures synthesized respectively in aqueous solution of SDS, PVP, or PVP–SDS supramolecular assemblies is schematically illustrated in Fig. 8. Process A and D are the illustrations of the growth mechanism of quasi-spheres in pure SDS and pure PVP solutions under microwave irradiation. The nascent gold nanocrystals formed at the early stages of the reactions were instantly protected by SDS or PVP, and after Ostwald ripening, they grew into the gold quasi-spheres. Process B and C are the illustrations of the growth mechanism of the elongate gold nanoparticles obtained under ordinary heating and the ginger-like gold nanobranches obtained under microwave irradiation. Under ordinary heating, the lower concentration of nascent nanocrystals slowly agglomerated into convex bumps, and the concave parts in the bumps were filled by gold atoms via Ostwald ripening and finally evolved into the elongate gold nanoparticles. However, under microwave irradiation, the higher concentration of nascent nanocrystals formed at the initial stages induced by microwave irradiation. When some of the nanocrystals approach one another closely enough, they are mutually attracted by van der Waals forces and extremely anxious hierarchically aggregated into the polybranches, which eventually evolved into the ginger-like nanobranches.

Conclusions

In this paper, ginger-like Au nanobranches are prepared in PVP–SDS aqueous solution under microwave irradiation through a one-pot, facile, rapid, and morphology-controlled synthesis route. Microwave irradiation is in favor of promoting irregular morphology through offering rapid and uniform heating to system, which makes abundant nascent gold nanocrystals occurred in solution in the initial stage of the reaction. Compared with templates of SDS or PVP, PVP–SDS supramolecular assemblies themselves have the hierarchical structure, which facilitates directing hierarchical assembly of gold nanocrystals. In the process of hierarchical assembly of gold nanobranches, the short-range order SDS-bound micelles act as the primary templates to mediate the tiny nanocrystals with diameters around 10 nm according to the micelle templates, and then the long-range order PVP–SDS supramolecular assemblies act as the secondary templates to fabricate several above gold nanocrystals within a limited space into elaborate gold nanostructures. Based on the experimental results, the possible growth mechanism of the ginger-like gold nanobranches is inferred to be a template-mediated and microwave-assisted hierarchical assembly via the unique co-effect of PVP–SDS soft template and microwave irradiation.

Acknowledgment The authors gratefully acknowledge support from the National Natural Science Foundation of China (no. 20871059).

References

1. Xu L, Li B, Jin Y (2011) Inner filter effect of gold nanoparticles on the fluorescence of quantum dots and its application to biological aminothiols detection. Talanta 84:558–564
2. Cobley CM, Chen J, Cho EC, Wang LV, Xia Y (2011) Gold nanostructures: a class of multifunctional materials for biomedical applications. Chem Soc Rev 40:44–56
3. Jain PK, Lee KS, El-Sayed IH, El-Sayed MA (2006) Calculated absorption and scattering properties of gold nanoparticles of different size, shape, and composition: applications in biological imaging and biomedicine. J Phys Chem B 110:7238–7248
4. Smith DK, Korgel BA (2008) The importance of the CTAB surfactant on the colloidal seed-mediated synthesis of gold nanorods. Langmuir 24:644–649
5. Kim F, Sohn K, Wu J, Huang J (2008) Chemical synthesis of gold nanowires in acidic solutions. J Am Chem Soc 130:14442–14443
6. Chu HC, Kuo CH, Huang MH (2006) Thermal aqueous solution approach for the synthesis of triangular and hexagonal gold nanoplates with three different size ranges. Inorg Chem 45:808–813
7. Yang G, Chen Y, Li L, Yang Y (2011) Direct electrochemical determination of morphine on a novel gold nanotube arrays electrode. Clin Chim Acta 412:1544–1549
8. Xu D, Gu J et al (2010) Development of chitosan-coated gold nanoflowers as SERS-active probes. Nanotechnology 21:375101. doi:10.1088/0957-4484/21/37/375101
9. Yuan H, Ma W, Chen C, Zhao J, Liu J, Zhu H, Gao X (2007) Shape and SPR evolution of thorny gold nanoparticles promoted by silver ions. Chem Mater 19:1592–1600
10. Liu M, Guyot-Sionnest P (2005) Mechanism of silver (I)-assisted growth of gold nanorods and bipyramids. J Phys Chem B 109:22192–22200
11. Kou X, Zhang S, Tsung C-K, Yeung MH, Shi Q, Stucky GD, Sun L, Wang J, Yan C (2006) Growth of gold nanorods and bipyramids using CTEAB surfactant. J Phys Chem B 110:16377–16383
12. Khoury CG, Vo-Dinh T (2008) Gold nanostars for surface-enhanced Raman scattering: synthesis, characterization and optimization. J Phys Chem C 112:18849–18859

13. Kuo CH, Huang MH (2005) Synthesis of branched gold nanocrystals by a seeding growth approach. Langmuir 21:2012–2016
14. Wu HL, Chen CH, Huang MH (2009) Seed-mediated synthesis of branched gold nanocrystals derived from the side growth of pentagonal bipyramids and the formation of gold nanostars. Chem Mater 21:110–114
15. Lim B, Camargo PHC, Xia Y (2008) Mechanistic study of the synthesis of Au nanotadpoles, nanokites, and microplates by reducing aqueous $HAuCl_4$ with poly(vinyl pyrrolidone). Langmuir 24:10437–10442
16. Pardias-Blanco I, Hoppe CE, Pieiro-Redondo Y, Lpez-Quintela MA, Rivas J (2008) Formation of gold branched plates in diluted solutions of poly(vinylpyrrolidone) and their use for the fabrication of near-infrared-absorbing films and coatings. Langmuir 24:983–990
17. Shen Q, Wei H, Wang L, Zhou Y, Zhao Y, Zhang Z, Wang D, Xu G, Xu D (2005) Crystallization and aggregation behaviors of calcium carbonate in the presence of poly(vinylpyrrolidone) and sodium dodecyl sulfate. J Phys Chem B 109:18342–18347
18. Esumi K, Iitaka M, Torigoe K (2000) Kinetics of simultaneous adsorption of poly(vinylpyrrolidone) and sodium dodecyl sulfate on alumina particles. J Colloid Interface Sci 232:71–75
19. Cao X, Yu F, Li L, Yao Z, Xie Y (2003) Copper nanorod junctions templated by a novel polymer-surfactant aggregate. J Cryst Growth 254:164–168
20. Ren Y, Xu C, Wu M, Niu M, Fang Y (2011) Controlled synthesis of gold nanoflowers assisted by poly(vinyl pyrrolidone)-sodium dodecyl sulfate aggregations. Colloids Surf, A: Physicochemical and Engineering Aspects 380:222–228
21. Liu F-K, Chang Y-C, Koa F-H, Chu T-C (2004) Microwave rapid heating for the synthesis of gold nanorods. Materials Letters 58:373–377
22. Hu X, Yu JC (2008) High-yield synthesis of nickel and nickel phosphide nanowires via microwave-assisted processes. Chem Mater 20:6743–6749
23. Sun X, Dong S, Wang E (2005) High-yield synthesis of large single-crystalline gold nanoplates through a polyamine process. Langmuir 21:4710–4712
24. Chen H, Kou X, Yang Z, Ni W, Wang J (2008) Shape- and size-dependent refractive index sensitivity of gold nanoparticles. Langmuir 24:5233–5237
25. Yang S, Wang Y, Wang Q, Zhang R, Yang Z, Guo Y, Ding B (2007) Growth of gold nanoplates: the case of a self-repair mechanism. Cryst Growth Des 7:2258–2261
26. Jiang WH, Han SJ (2000) Viscosity of nonionic polymer/anionic surfactant complexes in water. J Colloid Interf Sci 229:1–5
27. Minatti E, Zanette D (1996) Salt effects on the interaction of poly (ethylene oxide) and sodium dodecyl sulfate measured by conductivity. Colloids Surf, A: Physicochemical and Engineering Aspects 113:237–246
28. Cosgrove T, Mears SJ et al (1999) Polymer, particle, surfactant interactions. Colloids Surf A 149:329–338
29. Bakshi MS, Possmayer F, Petersen NO (2008) Aqueous-phase room-temperature synthesis of gold nanoribbons: soft template effect of a gemini surfactant. J Phys Chem C 112:8259–8265
30. Kuo C-H, Chiang T-F, Chen L-J, Huang MH (2004) Synthesis of highly faceted pentagonal- and hexagonal-shaped gold nanoparticles with controlled sizes by sodium dodecyl sulfate. Langmuir 20:7820–7824
31. Zhou M, Chen S, Zhao S (2006) Synthesis of icosahedral gold nanocrystals: a thermal process strategy. J Phys Chem B 110:4510–4513
32. Mafun F, Kohno J, Takeda Y, Kondow T, Sawabe H (2000) Formation and size control of silver nanoparticles by laser ablation in aqueous solution. J Phys Chem B 104:9111–9117
33. Soejima T, Kimizuka N (2009) One-pot room-temperature synthesis of single-crystalline gold nanocorolla in water. J Am Chem Soc 131:14407–14412
34. Golan Y, Margulis L, Rubinstein I, Hodes G (1992) Epitaxial electrodeposition of cadmium selenide nanocrystals on gold. Langmuir 8:749–752
35. Krishnakumar T, Jayaprakash R, Pinna N, Singh VN, Mehta BR, Phani AR (2009) Microwave-assisted synthesis and characterization of flower shaped zinc oxide nanostructures. Materials Letters 63:242–245
36. Xie J, Zhang Q, Lee JY, Wang DIC (2008) The synthesis of SERS-active gold nanoflower tags for *in vivo* applications. ACS Nano 2:2473–2480